The mechanics-modulated tunneling spectrum and low-pass effect of viscoelastic molecular monolayer

Yun Chen, Xiaoyue Zhang, Jian Shao, Jing Yu, Biao Wang, and Yue Zheng

Citation: AIP Advances **7**, 105326 (2017); doi: 10.1063/1.5003766
View online: https://doi.org/10.1063/1.5003766
View Table of Contents: http://aip.scitation.org/toc/adv/7/10
Published by the American Institute of Physics

The mechanics-modulated tunneling spectrum and low-pass effect of viscoelastic molecular monolayer

Yun Chen,[1,2] Xiaoyue Zhang,[1,2,3,a] Jian Shao,[1,2] Jing Yu,[1,2] Biao Wang,[1,2,3,b] and Yue Zheng[1,2,c]

[1]*State Key Laboratory of Optoelectronic Materials and Technologies, Sun Yat-sen University, Guangzhou 510275, China*

[2]*Micro&Nano Physics and Mechanics Research Laboratory, School of Physics, Sun Yat-sen University, Guangzhou 510275, China*

[3]*Sino-French Institute of Nuclear Engineering and Technology, Sun Yat-sen University, Zhuhai 519082, China*

(Received 7 September 2017; accepted 24 October 2017; published online 31 October 2017)

Understanding the force-induced conductance fluctuation in molecules is essential for building molecular devices with high stability. While stiffness of molecule is usually considered to be desirable for stable conductance, we demonstrate mechanical dragging in viscoelastic molecules integrates both noise resistance and mechanical controllability to molecular conductance. Via conductive atomic force microscope measurement and theoretical modeling, it's found that viscoelastic Azurin monolayer has spectrum-like pattern of conductance corresponding to the duration and strength of applied mechanical pulse under low-frequency excitation. Conductance fluctuation is prevented under high-frequency excitation by dragging dissipation, which qualifies molecular junction with electric robustness against mechanical noise. https://doi.org/10.1063/1.5003766

I. INTRODUCTION

Molecular electronics aims to build electrical components using individual or ensemble molecules.[1] This promising technique meets the increasing demands for miniaturization of electronic components such as diode, memory and switching,[2–5] and provides an ideal carrier for achieving highly functional devices that responds to mechanical force, thermal effects, optic effects, etc.[6–10] Mechanical force can influence molecular conductance by initiating structural phase transition, affecting the molecule-electrode interaction and introducing deformation of molecular junctions.[11–14] Among these cases, deformation-induced conductance fluctuation has been spotlighted because it is a universal effect that independent on the chemical component.[15,16]

Since the tunneling current of the molecular junction is exponential correlated with the electrode-to-electrode distance,[17] the molecule conductance should be very sensitive to the deformation. Therefore, it is usually considered that molecules with high stiffness (such as alkane) have stable conductance under mechanical load, and conductance of low stiffness molecules (such as bio-marcomolecules) are more easily influenced by force. Most of previous studies investigate this subject via static and quasi-static measurements, and might not be comprehensive under dynamic loading especially for viscoelastic bio-marcomolecules. Viscoelasticity exists widely in bio-marcomolecules, which is caused by the dragging and restoring force between coiled backbones.[15] The dragging effect generates time-dependent structural change instead of instantaneous

[a]Corresponding author should be addressed to zhangxy26@mail.sysu.edu.cn
[b]Electronic address: wangbiao@mail.sysu.edu.cn
[c]Electronic address: zhengy35@mail.sysu.edu.cn

deformation under force. Thus dynamic behaviors such as damped vibrating and frequency-limited response can be observed in viscoelastic molecules.[18] The influences of these dynamic effects on response of molecular conductance have not been explored. Clarifying the issue will provide new insights into the understanding of mechanical controllability and stability of electric properties of molecule.

In view of these considerations, we conduct an indepth study on the conductance response of viscoelastic molecules under dynamic loads. The conductance response of bio-marcomolecule monolayer under mechanical pulse is characterized via conductive atomic force microscopy (CAFM). Theoretical model for conductance response of viscoelastic molecule under mechanical stimuli is developed to explore the time-dependent effect. The influence of mechanical properties of molecular monolayer on the conductance response has also been analyzed and summarized.

II. EXPERIMENT

An electron-mediating protein Azurin (Az) is used as the sample for characterizing the dynamic conductance response in bio-macromolecule. Az monolayer was obtained by immersing an atomic flat Au substrate in 5μM Az (Sigma A3672) solution in acetate buffer for at least 2 hours, followed by thorough rinsing with ultrapure water and blown dry with nitrogen. The thickness of Az monolayer was 2.74±0.45nm, which approved there was only one layer of molecules on substrate. To obtain the force-induced conductance response of Az monolayer, we measured the *I-t* curves of the sample using CAFM (CSPM 5500, Being Co. Ltd) and a pyramid gold-coated probe with 0.2N/m force constant. In the measurement, the input voltage for vertical channel of scanner was controlled to cycle with period of 10000ms, which induced a triangular mechanical pulse with peak force of 30nN on Az monolayer. Meanwhile, 0.5V bias was applied between the tip and substrate. And the current signal as well as tip force during the loading cycle were recorded and illustrated as function of time. Typical result is shown in Fig. 1. Rather than increased synchronously with tip force, the current reached its peak value after the unloading phase begins. As the force decreased, current signal maintained for about 1s and then vanished. The time-delayed characteristic makes the conductance response of Az under force like a kind of memory behavior. This memory-like pattern indicates the structural change in Az lags behind mechanical load and is able to restore after the force is withdraws. Lagging and restoration are the two main features of dynamic deformation in viscoelastic molecules, which evidence the strong connection between the dynamic conductance response and viscoelasticity of Az.

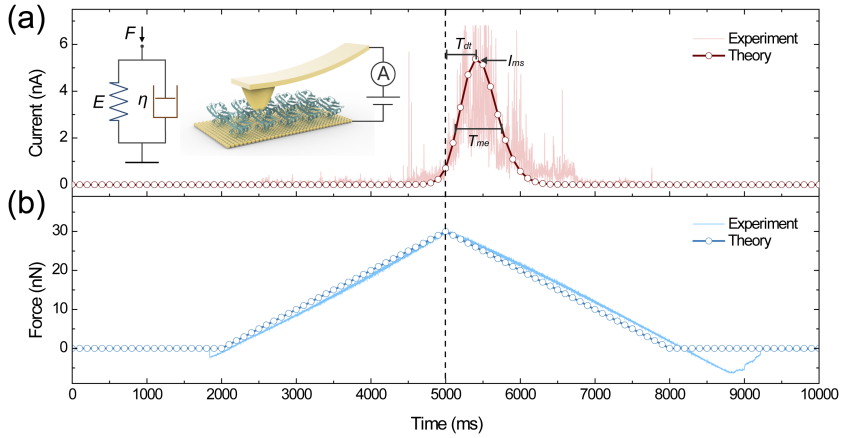

FIG. 1. (a) The *I-t* curves of Az monolayer under triangular pulse, in which red line with circles represents the theoretical *I-t* curve and the one without circle is experimental one. (b) The mechanical pulse showed as the blue lines. Inset: the schematic diagram of CAFM measurements and the Kelvin–Voight model for Az monolayer.

III. THEORETICAL MODEL

To constitute the theoretical model of this memory behavior, we adopt Kelvin-Voigt model to describe the deformation of Az monolayer under tip force. The dynamic response of Az is given as $Ex + \eta\dot{x} = F(t)$, where $F(t)$ is the tip force, x is the normal displacement of the monolayer, t is time, E and η are the stiffness and viscous drag coefficient respectively. This model well explains the lagging and restoration in bio-marcomolecules by introducing the internal restoring force Ex and dragging force, $\eta\dot{x}$[18,19] thus it is suitable for our case. Following the CAFM experiment, $F(t)$ can be written as $F(t) = \begin{cases} kt, & (0 \le t < T/2) \\ -kt + kT, & (T/2 \le t \le T) \end{cases}$, where k represents load rate and T is load period. By substituting $F(t)$ into Kelvin-Voigt model, $x(t)$ can then be solved as,

$$x(t) = \begin{cases} \dfrac{k\eta}{E^2} e^{-\frac{Et}{\eta}} + \dfrac{k}{E}t - \dfrac{k\eta}{E^2}, & \left(0 \le t < \frac{T}{2}\right) \\ \left(\dfrac{k\eta}{E^2} - \dfrac{2k\eta}{E^2} e^{\frac{ET}{2\eta}}\right) e^{-\frac{Et}{\eta}} + \dfrac{k}{E}\left(T - t\right) + \dfrac{k\eta}{E^2}, & \left(\frac{T}{2} \le t \le T\right) \end{cases} \tag{1}$$

The tunneling current in Az monolayer can be given by Simmons tunneling model,[20,21]

$$I = \frac{eD^2}{16\pi\hbar d^2} \left\{ \left(\Phi - \frac{eV}{2}\right) \exp\left[-\frac{2(2m)^{\frac{1}{2}}}{\hbar} \left(\Phi - \frac{eV}{2}\right)^{\frac{1}{2}} d \right] - \left(\Phi + \frac{eV}{2}\right) \exp\left[-\frac{2(2m)^{\frac{1}{2}}}{\hbar} \left(\Phi + \frac{eV}{2}\right)^{\frac{1}{2}} d \right] \right\} \tag{2}$$

where barrier height Φ and barrier thickness d are the two structural factors affecting the conductance, D is the diameter of contact area, V is applied voltage, e and m are the charge and effective mass of electron, respectively. For Au/Az/Au junction, the barrier thickness is equivalent to the thickness of Az monolayer.[22,23] When the monolayer is compressed by tip force, the barrier thickness d_0 is reduced to $d(t) = d_0 - x(t)$, which causes the conductance fluctuation. During the compression, barrier height Φ decreases with the decrease of barrier thickness because of the atoms compacting,[24] which also contributes to the conductance response.

IV. RESULTS AND DISCUSSIONS

In order to verify our theoretical model, a numerical calculation has been performed to simulate the conductance response of Az monolayer under triangular pulses. The initial thickness of Az monolayer before loading is $d_0 = 3 \times 10^{-9}\ m$. The load period is set to $T = 6000ms$ according to the contact time of the AFM tip and the monolayer shown in the Force-Distance curve (Fig. 1(b)). The peak force is $30nN$, implying the loading rate $k = 1 \times 10^{-8}\ N/s$. In the CAFM tests, the conductive tip has a curvature radius of $25nm$, which gives approximately $D \approx 20nm$. For the other physical constants, $\hbar = 1.0546 \times 10^{-34} J \cdot s$, $m = 9.1094 \times 10^{-31} kg$ and $e = 1.6 \times 10^{-19} C$ are used in the calculation. The value of barrier height of Az can be given by $\Phi = 0.15017 + 8.065 \times 10^7\ d(t)$ according to static data from previous article.[25] As illustrated in Fig. 1, theoretical *I-t* curve is in good agreement with the experimental data under fitted parameters $E = 14.7\ N/m$ and $\eta = 9N \cdot s/m$. And it succeeds in reproducing the memory-like behavior of conductance response in Az, which demonstrates the influences of viscoelasticity and validates our model. According to the fitted values of E and the curvature radius of CAFM tip, the Young's modulus of Az monolayer can be estimated to be 110MPa, which is within the range of bio-macromolecules reported by bulk determinations (1-2500MPa) and is close to fibrillin or globular proteins like lactate oxidase.[26,27] The drag coefficient η gives a kinetic viscosity coefficient of 3GPa · s, which is closed to organic polymer such as polyvinylidene fluoride (24GPa · s).[28] Both of the estimations show the parameters E and η deduce mechanical coefficients within reasonable range, proving the fitted values are appropriate.

Three key variables are defined to characterize the memory behavior of Az monolayer, which are peak-current as memory strength I_{ms}, half-peak width of current as memory endurance T_{me}, and

the interval time between peak force and peak current as delay time T_{dt}. These three key variables can be solved from Eq. (1)–(2) as:

$$T_{dt} = \frac{\eta}{E}\ln\left(2e^{\frac{ET}{2\eta}} - 1\right) - \frac{T}{2} \tag{3}$$

$$I_{ms} = I(T_{dt} + \frac{T}{2}) = \frac{D^2\hbar e}{16\pi}\left\{d_0 - \left\{\left(\frac{k\eta}{E^2} - \frac{2k\eta}{E^2}e^{\frac{ET}{2\eta}}\right)e^{-\ln\left(2e^{\frac{ET}{2\eta}}-1\right)} + \frac{k}{E}\left[T - \frac{\eta}{E}\ln\left(2e^{\frac{ET}{2\eta}} - 1\right)\right] + \frac{k\eta}{E^2}\right\}\right\}^{-2}$$
$$\times\left\{\left(\Phi - \frac{eV}{2}\right)\exp\left\{-\frac{2(2m)^{\frac{1}{2}}}{\hbar}\left(\Phi - \frac{eV}{2}\right)^{\frac{1}{2}}\left\{d_0 - \left\{\left(\frac{k\eta}{E^2} - \frac{2k\eta}{E^2}e^{\frac{ET}{2\eta}}\right)e^{-\ln\left(2e^{\frac{ET}{2\eta}}-1\right)}\right.\right.\right.$$
$$\left.\left.\left. + \frac{k}{E}\left[T - \frac{\eta}{E}\ln\left(2e^{\frac{ET}{2\eta}} - 1\right)\right] + \frac{k\eta}{E^2}\right\}\right\} - \left(\Phi + \frac{eV}{2}\right)\exp\left\{-\frac{2(2m)^{\frac{1}{2}}}{\hbar}\left(\Phi + \frac{eV}{2}\right)^{\frac{1}{2}}\right.$$
$$\left.\times\left\{d_0 - \left\{\left(\frac{k\eta}{E^2} - \frac{2k\eta}{E^2}e^{\frac{ET}{2\eta}}\right)e^{-\ln\left(2e^{\frac{ET}{2\eta}}-1\right)} + \frac{k}{E}\left[T - \frac{\eta}{E}\ln\left(2e^{\frac{ET}{2\eta}} - 1\right)\right] + \frac{k\eta}{E^2}\right\}\right\}\right\}\right\} \tag{4}$$

$$T_{me} = |t_2 - t_1| \tag{5}$$

where t_1 and t_2 are the two roots of equation $I(t) = \frac{1}{2}I_{ms}$. The memory characteristics of Az under different peak force and load period have been analyzed and illustrated in Fig. 2. Peak force has great influence on I_{ms} (Fig. 2(a) and 2(b)). With 6s load period and 0.5V applied voltage, I_{ms} rapidly enhances about 35 times when the peak force is increased from 24nN to 30nN. Meanwhile, T_{me} and T_{dt} are barely affected. In addition to the magnitude of force, conductance of Az monolayer is also found to respond to the duration of the mechanical pulse (Fig. 2(c) and 2(d)). Under the same peak force of 30nN, I_{ms} with load period of 2s increase from 0.002nA to 5.4nA with load period of 6s. Meanwhile, T_{me} and T_{dt} are 87% and 16% longer. These results are in correspondence with our previous experimental observations.[16] As shown in Fig. S1 and Fig. S2 of supplementary material,

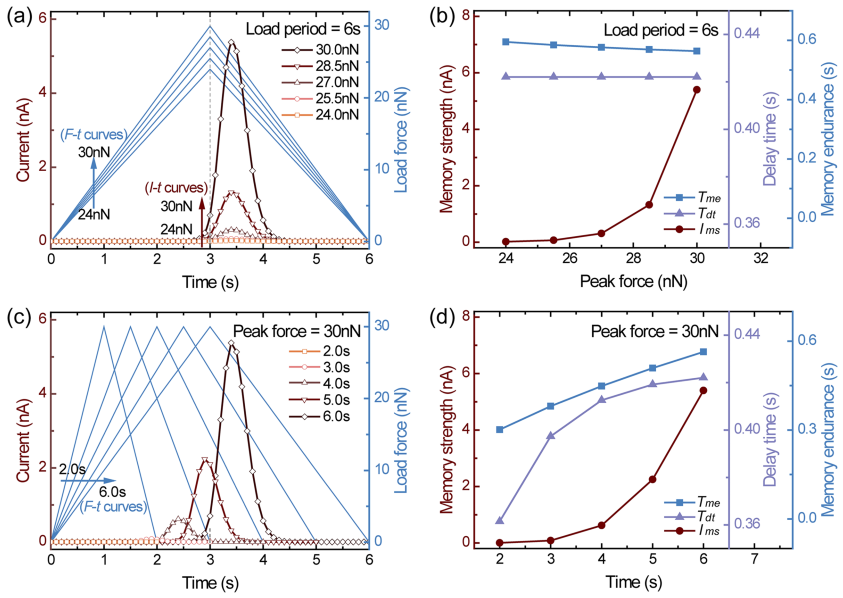

FIG. 2. Influences of load parameters on memory characteristics. (a) *I-t* and *F-t* curves with different peak force from 24.0nN to 30.0nN with a fixed load period of 6s. (b) The dependence of T_{me}, T_{dt} and I_{ms} on peak force. (c) *I-t* and *F-t* curves with different load period from 2.0s to 6.0s under fixed peak force of 30nN. (d) The corresponding T_{me}, T_{dt} and I_{ms} under different load period.

the controllability of Az conductance response under different peak force and load period have been demonstrated via CAFM measurements using spherical tip with a curvature radius of $1\mu m$. Our model is able to reproduce these data with mechanical parameters $E_s = (\frac{\alpha D_s}{D})^2 E$ and $\eta_s = (\frac{\beta D_s}{D})^2 \eta$, where D_s is the contact diameter between the spherical tip and monolayer according to Hertz model, α, $\beta = 1 \pm 0.35$ are correction factors that corresponding to the uncertainness of tip-sample contact. The impure peaks in Fig. S1 of the supplementary material are also caused by the influence of large contact area under spherical tip and the morphology fluctuation of Az monolayer. The effect of load period introduces extra control method to the molecular conductance. In the case that only the magnitude of conductance response is concerned, certain I_{ms} can be aroused by either short mechanical pulse with high peak force or weak pulse with long load period. Accordingly, Az monolayer can acts as a logical OR gate. Furthermore, even though different pulses could produce the same I_{ms}, longer load period will results in longer T_{me} and T_{dt}. Therefore, in case all three key variables are considered, Az monolayer has unique time-resolved pattern of *I-t* curve for certain mechanical pulse. We define this spectrum like *I-t* curve that triggered by dynamic load as mechanics-modulated tunneling spectrum (MTS). The diversiform MTS under different mechanical pulses reflect the multi-state characteristic of memory behavior in Az monolayer.

One important conclusion of above calculation is that mechanical pulse with shorter load period will result in MTS with smaller I_{ms}. This is because the internal dragging force retards the structural change of molecule. The insensitivity of Az conductance under short period mechanical pulse implies the electric stability against high frequency mechanical noise. To reveal this property, Az MTS under combined load consisting of triangular pulse and sinusoidal noise have been calculated. As shown in Fig. 3(a), sinusoidal noise with amplitude A = 5nN and frequency f = 5Hz induces obvious deviation to original MTS under pure triangular pulse. The current fluctuation is about 2nA. With higher frequency f = 20Hz (Fig. 3(b)), the current fluctuation is reduced to 0.25nA, which is insignificant compared to 5nA peak current in original MTS. Our results prove that conductance of viscoelastic Az is robust against high-frequency excitation. At the same time, it is controllable with low-frequency load. This property is analogous to the low-pass effect in RC circuits, which provides a new strategy for anti-interference in molecular junction instead of choosing high stiffness molecules and sacrifices mechanical controllability.

The dependence between MTS and applied voltage has been studied and summarized in Fig. 4. By fixing peak force to 30nN and considering load period as independent variable, I_{ms} under different applied voltage from 0.1V to 2.0V have been calculated (Fig. 4(a)). While overall I_{ms} under 2V are several orders of magnitude higher than that under 0.1V, I_{ms} variation between load period of 1s and 6s is one orders of magnitude higher under 0.1V. A similar pattern is validated with fixed load

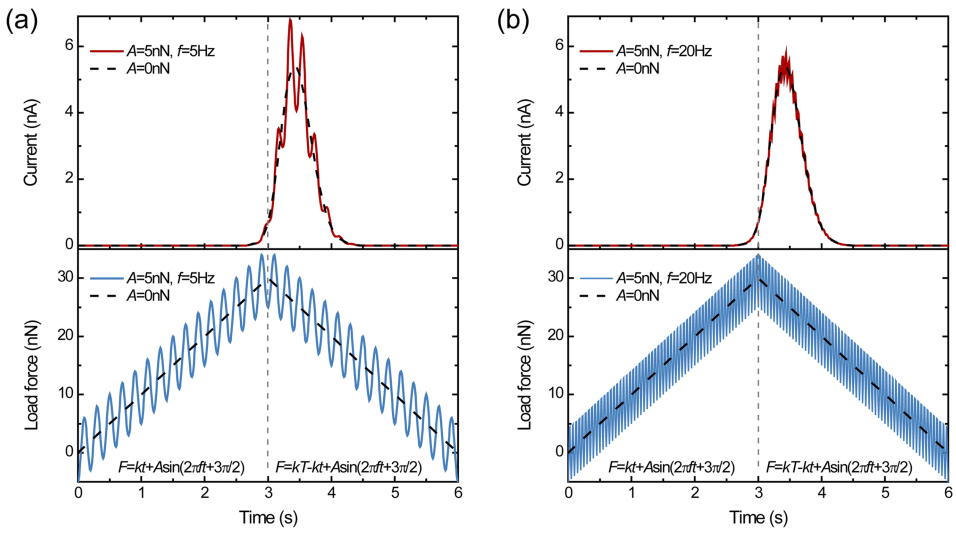

FIG. 3. MTS under combination of triangular pulse and sinusoidal noise with (a) 5Hz and (b) 20Hz.

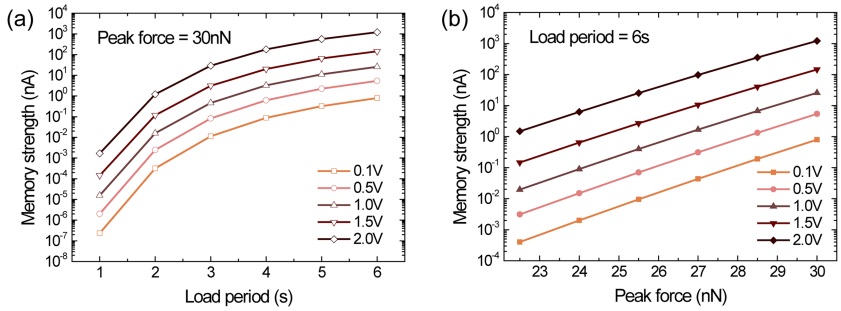

FIG. 4. Memory strength under different bias voltage from 0.1V to 2.0V, when (a) peak force is fixed to 30nN and (b) load period is anchored to 6s, respectively.

period and considering peak force as independent variable (Fig. 4(b)). Consequently, MTS has strong signal under high voltage. And the controllable range of MTS is broader under lower voltage, which therefore enhance the low-pass effect.

Since the memory behavior and low-pass effect of Az is origin from viscoelasticity, similar phenomena must exist in other viscoelastic molecules as well. A nature question is that how will the mechanical properties of different viscoelastic molecules affect the stability and controllability of their conductance. To address this issue, we investigate the influence of stiffness E and viscous drag coefficient η on MTS. For a certain molecule, Φ and d_0 can be obtained via I-V measurement and AFM scanning, respectively. Thus they are treated as known parameters in the following analysis. And their values in Az are used for instantiation. Under triangular pulse with load period of 6s and peak force of 30nN, the influence of E and η on MTS has been calculated and shown in Fig.5. With 13.3% higher stiffness, I_{ms} and T_{dt} decrease by 94.4% and 11.6%, but the change in T_{me} is neglectable (Fig. 5(a)). When the viscous coefficient is increased from 9N · s/m to 13N · s/m, I_{ms} reduces 84.7%. Meanwhile T_{me} and T_{dt} is 17.5% and 41.8% higher, respectively (Fig. 5(b)). More comprehensive results are presented in 3D graphics of I_{ms}, T_{me} and T_{dt} as functions of both E and η in Fig. 5(c)–(e). Molecules with higher stiffness undergo less deformation and quicker restoration, which limits the variation and time-delayed characteristic of conductance response. Higher viscous drag coefficient also reduces deformation and I_{ms}. In contrast to stiffness, it takes longer time for the molecule to restore so that T_{me} and T_{dt} are lengthened. These data are helpful for utilizing viscoelastic molecules to fabricate functional molecular devices. For example, molecules with high η can store the information of mechanical force for significant duration, which make it suitable for building mechanics-modulated multi-state memory.

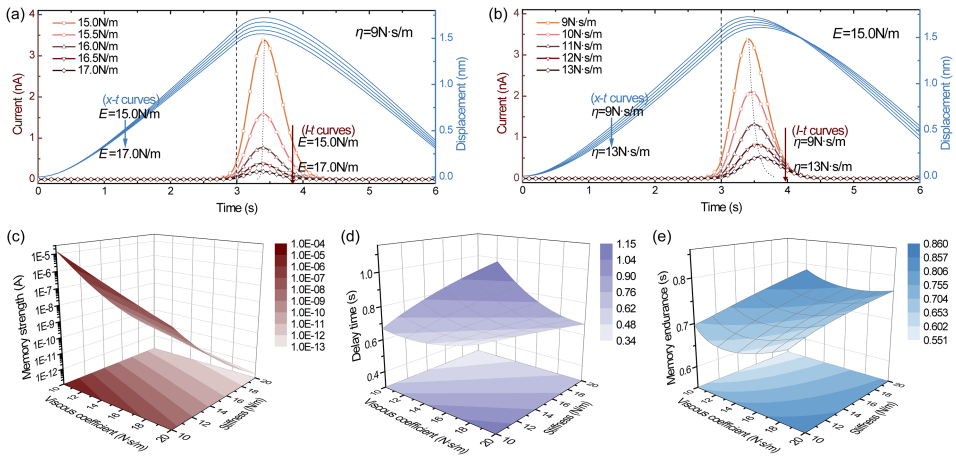

FIG. 5. The current and displacement under triangular pulse with (a) different stiffness and (b) viscous coefficient. 3D graphs of (c) I_{ms}, (d) T_{dt} and (e) T_{me} as the function of stiffness and viscous coefficient.

V. CONCLUSIONS

In summary, the force-induced conductance response in viscoelastic molecules is studied. By proposing the concept of MTS, we demonstrate conductance of viscoelastic Az monolayer responds to both duration and strength of low-frequency mechanical pulse. It is further revealed that internal dragging force prevents conductance fluctuation under high-frequency excitations, bringing Az monolayer the robustness against high-frequency mechanical noise. The influences of voltage and mechanical properties on MTS have also been explored, which shows the dragging effect in viscoelastic molecules plays an important role in potential applications such as molecular multi-state memory.

SUPPLEMENTARY MATERIAL

See supplementary material for the experimental and theoretical results of controllability of Az conductance response under different peak force and load period.

ACKNOWLEDGMENTS

The authors gratefully acknowledge the financial support of NSFC (Nos. 11402312, 11474363, 11232015, 11672339), Guangzhou science and technology project (No. 201707020002). Xiaoyue Zhang also thanks support by the Fundamental Research Funds for the Central Universities to Micro&Nano Physics and Mechanics Research Laboratory.

[1] D. Xiang, X. L. Wang, C. C. Jia, T. Lee, and X. F. Guo, Chem. Rev. **116**(7), 4318 (2016).
[2] T. S. Arrhenius, M. Blanchard-Desce, M. Dvolaitzky, J.-M. Lehn, and J. Malthete, Proc. Nat. Acad. Sci. **83**(15), 5355 (1986).
[3] C. A. Nijhuis, W. F. Reus, J. R. Barber, M. D. Dickey, and G. M. Whitesides, Nano Lett. **10**(9), 3611 (2010).
[4] M. Irie, Chem. Rev. **100**(5), 1685 (2000).
[5] B. L. Feringa, Acc. Chem. Res. **34**(6), 504 (2001).
[6] J. F. Zhou, F. Chen, and B. Q. Xu, J. Am. Chem. Soc. **131**(30), 10439 (2009).
[7] C. Meng, P. Huang, J. W. Zhou, C. K. Duan, and J. F. Du, Chin. Phys. Lett. **32**(7) (2015).
[8] S. V. Aradhya and L. Venkataraman, Nat. Nanotechnol. **8**(6), 399 (2013).
[9] H. Vazquez, R. Skouta, S. Schneebeli, M. Kamenetska, R. Breslow, L. Venkataraman, and M. S. Hybertsen, Nat. Nanotechnol. **7**(10), 663 (2012).
[10] A. N. Pasupathy, R. C. Bialczak, J. Martinek, J. E. Grose, L. A. K. Donev, P. L. McEuen, and D. C. Ralph, Science **306**(5693), 86 (2004).
[11] T. Kim, Z. F. Liu, C. Lee, J. B. Neaton, and L. Venkataraman, Proc. Nat. Acad. Sci **111**(30), 10928 (2014).
[12] Z. F. Huang, F. Chen, P. A. Bennett, and N. J. Tao, J. Am. Chem. Soc. **129**(43), 13225 (2007).
[13] C. Bruot, J. Hihath, and N. J. Tao, Nat. Nanotechnol. **7**(1), 35 (2012).
[14] J. Shao, X. Y. Zhang, Y. Chen, and Y. Zheng, npj Compu. Mat. **2**, 1 (2016).
[15] E. Leary, M. T. Gonzalez, C. Van Der Pol, M. R. Bryce, S. Filippone, N. Martín, and N. Agraït, Nano Lett. **11**(6), 2236–2241 (2011).
[16] X. Y. Zhang, J. Shao, Y. Chen, W. J. Chen, J. Yu, B. Wang, and Y. Zheng, Phys. Chem. Chem. Phys. **19**(9), 6757 (2017).
[17] S. E. Lyshevski, *Nano and molecular electronics handbook* (CRC Press, Boca Raton, FL, 2016).
[18] N. Özkaya, D. Leger, D. Goldsheyder, and M. Nordin, *Fundamentals of biomechanics: Equilibrium, motion, and deformation* (Springer International Publishing, Cham, 2017).
[19] R. Berkovich, R. I. Hermans, I. Popa, G. Stirnemann, S. Garcia-Manyes, B. J. Berne, and J. M. Fernandez, Proc. Nat. Acad. Sci **109**(36), 14416 (2012).
[20] J. G. Simmons, J. Appl. Phys. **34**(6), 1793 (1963).
[21] J. W. Zhao, J. J. Davis, M. S. P. Sansom, and A. Hung, J. Am. Chem. Soc. **126**(17), 5601 (2004).
[22] A. V. Pakoulev and V. Burtman, J. Phys. Chem. C **113**(51), 21413 (2009).
[23] J. F. Zhou and B. Q. Xu, Appl. Phys. Lett. **99**(4) (2011).
[24] C. C. Page, C. C. Moser, X. Chen, and P. L. Dutton, Nature **402**, 47 (1999).
[25] J. J. Davis, N. Wang, A. Morgan, T. T. Zhang, and J. W. Zhao, Faraday Discuss. **131**, 167 (2006).
[26] M. Guthold, W. Liu, E. A. Sparks, L. M. Jawerth, L. Peng, and M. Falvo, Cell Biochem. Biophys. **49**(3), 165–181 (2007).
[27] A. Parra, E. Casero, E. Lorenzo, F. Pariente, and L. Vázquez, Langmuir. **23**(5), 2747–54 (2007).
[28] S. A. Hackney, K. E. Aifantis, A. Tangtrakarn, and S. Shrivastava, Mater. Sci. Tech. **28**(9-10), 1161 (2013).